Glycoconjugate Journal 21, 111–123, 2004
© 2004 Kluwer Academic Publishers. Manufactured in The Netherlands.

Carbohydrate-carbohydrate interaction as a major force initiating cell-cell recognition

Iwona Bucior[1,2] and Max M. Burger[1,2]

[1] *Friedrich Miescher Institute, Novartis Research Foundation, Maulbeerstrasse 66, 4058 Basel, Switzerland,*
[2] *Marine Biological Laboratories, 7 MBL Street, Woods Hole, MA 02543, USA*

Sponges were the earliest multicellular organisms to evolve through the development of cell recognition and adhesion processes mediated by cell surface proteoglycans. Information on sponges has an extra added value because, as a group, they are the oldest Metazoans alive and contribute more to our understanding of life on earth than knowledge of other animal groups. Although the proteoglycans are emerging as key players in various physiological and pathophysiological cellular events, little is known about the carbohydrate moiety of the proteoglycan molecule. Until recently there was no evidence provided for the existence of specific and biologically significant carbohydrate-carbohydrate interaction. We show here that the interaction between single oligosaccharides of surface proteoglycans is relatively strong (in the 200–300 piconewtons range) and in the same range as other relevant biological interactions, like those between antibodies and antigens. This carbohydrate-carbohydrate recognition is highly species-specific and perfectly mimics specific cell-cell recognition. Both the strength and the species-specificity of the carbohydrate-carbohydrate interaction are guaranteed by polyvalency, by compositional and architectural differences between carbohydrates, and by the arrangement of the carbohydrate chain in a three-dimensional context. Ca^{2+}-ions are essential and probably provide coordinating forces. Our findings confirm the existence and character of species-specific carbohydrate-carbohydrate recognition fundamental to cell recognition and adhesion events.
Published in 2004.

Keywords: **cell-cell recognition, cell surface proteoglycan, carbohydrate composition, carbohydrate-carbohydrate interaction, species-specificity, adhesion force**

Abbreviations: **AFM, atomic force microscopy; pN, piconewtons; CSW, calcium-and magnesium-free Tris-buffered seawater; artificial seawater; Le^x, $Lewis^x$ determinant (Galβ1 → 4[Fucα1 → 3]GlcNAcβ1 → 3Galβ1 → 4Glcβ); TFA, trifluoroacetic acid.**

Introduction

Studies of the molecular recognition of carbohydrates are at a crossroads similar to that of the nucleic acids and peptides a few decades ago. Interest in carbohydrates has increased parallel to improvements in methods for their separation and analysis and the biological functions of these compounds are now being defined. It is well established that signaling and recognition involve protein-protein and/or carbohydrate-protein interactions. Direct carbohydrate-carbohydrate interactions are in general considered to be weak and not able to provide sufficient strength and specificity for cellular recognition. However, the definition of "weak interaction" is rather arbitrary and based upon the binding strength shown by carbohydrates during the extensive washing in such procedures as direct binding to cells, affinity chromatography, or detection by blotting [1,2]. More recent measurements of the forces between individual surface oligosaccharides of sponge proteoglycan molecules have shown that interaction can not only be as strong but also as specific as, for example, that between antibody and antigen [3].

Carbohydrates can operate at cell surfaces, where they often occur as components of glycoproteins [4], glycolipids [5], or proteoglycans [6] anchored in the cell membrane. The composition of glycolipids at the cell surface is strongly correlated with embryonic cell developmental stages and can serve as mediators of the crosstalk between tumor cells and host cells [7,8] Interaction of these glycolipids with receptors on other cell surfaces plays a signaling and regulatory role in cell

To whom correspondence should be addressed: Max M. Burger, Novartis Science Board, Novartis International AG, WKL-125.13.02, 4002 Basel, Switzerland. Tel.: +41-61 696 7690; E-mail: max.burger@group.novartis.com

development and adhesion [9,10]. These interactions involve carbohydrate-carbohydrate recognition and are dependent on divalent cations such as calcium (Ca^{2+}) and magnesium. For example, compaction of the mouse embryo at the morula stage [11,12] and the aggregation of mouse embryonic cells [12] occur as a result of recognition between Lewis^x trisaccharide structures in a Ca^{2+}-mediated association.

Proteoglycans are found in all connective tissues, in the extracellular matrix, and on the surfaces of virtually all animal cells. Despite their structural and functional diversity [13], proteoglycans have a general propensity to be extracellular matrix components, mediating specific matrix interactions and biological activities related to cell adhesion [14] via their carbohydrate chains or core proteins. However, it could not be resolved until recently whether the specificity of proteoglycan-mediated cell adhesion events resigns in a protein-carbohydrate or in a carbohydrate-carbohydrate interaction.

The first experimental demonstration of cell recognition and adhesion phenomena in the animal kingdom involved cell surface proteoglycan [15] of invertebrates, *i.e.* from the marine sponge model system [16]. Sponges are the simplest and earliest multicellular organisms. Remarkably, dissociated sponge cells from two different species can reaggregate through surface proteoglycans by species-specific associations that approach the selectivity of the evolutionarily advanced Ig superfamily. Consequently, this simple and highly specific cellular recognition phenomenon has been used for almost a century as a model system to study specific cellular recognition and adhesion during tissue and organ formation in multicellular organisms.

Specific cell-cell adhesion in most multicellular animals is mediated by two distinct classes of molecules: a Ca^{2+}-independent activity typical of the glycoproteins from the Ig superfamily [17], and Ca^{2+}-dependent cell-cell adhesion, the best example being the cadherins [18]. Interestingly, sponge proteoglycans reunite both functions in the same molecule and mediate species-specific cell-cell recognition via two functionally distinct domains: (1) a Ca^{2+}-independent cell-binding domain and (2) a Ca^{2+}-dependent self-association domain, which provide the intercellular adhesion force.

Sponge proteoglycans [19], otherwise known as aggregation factors (AFs), are large molecules with approximate molecular weights ranging from 2×10^4 kDa [20] to 1.4×10^6 kDa [21]. Based on atomic force microscope (AFM) images [22], proteoglycan molecules show either a linear or a sunburst-like core structure with 20–25 radiating arms. The best analyzed proteoglycan of *Microciona prolifera* carries two N-linked glycan molecules: one with a mass of 6.3 kDa present in the arms of the proteoglycan molecule that binds to a cell surface receptor independently of Ca^{2+} ions [23], and one with a mass of ~200 kDa and present in the core structure that self associates in a Ca^{2+}-dependent manner [24]. Carbohydrate moiety participation in the adhesion process was anticipated after it was found that glycosidase treatment [25] and periodate oxidation [26] destroyed the aggregation activity of proteoglycan molecules. Glass aminopropyl beads coated with protein-free 200-kDa glycan showed a Ca^{2+}-dependent aggregation equivalent to that of proteoglycan-coated beads [24]. The biological specificity and selectivity of the glycan-glycan interaction could then, however, not yet be proven. The monoclonal antibody raised against the purified surface proteoglycan of *Microciona prolifera* blocked cell aggregation, for which the epitopes were identified as short carbohydrate units of the 200-kDa glycan: a sulfated disaccharide [27] and a pyruvylated trisaccharide [28]. The concept of self-recognition of defined carbohydrate epitopes was confirmed using surface plasmon resonance to mimic the role of carbohydrates in cellular adhesion of *Microciona* [29]. The results showed self-recognition of the sulfated disaccharide and this event was proposed as a major force behind Ca^{2+}-dependent cell-cell recognition. Nevertheless, the biological relevance, *i.e.* the species-specific character of interactions between 200-kDa glycan molecules in sponges has been investigated only recently. It was shown for the first time that direct carbohydrate-carbohydrate interaction is highly species-specific and can play a major role in proteoglycan-mediated cellular recognition and adhesion events.

Here, we elaborate on recently published investigations on the strength and species-specific character of direct carbohydrate-carbohydrate interaction [3] and extend these studies. The 200-kDa glycans from core structures of four sponge species (*Microciona prolifera*, *Halichondria panicea*, *Suberites fuscus* and *Cliona celata*) were purified and their species-specific carbohydrate compositions revealed. In functional self-assembly cells, cells and glycan-coated beads, glycan-coated carboxylate-modified beads displayed species-specific recognition. Finally, atomic force microscopy (AFM) measurements of the forces between single 200-kDa glycan molecules from *Microciona* proteoglycan revealed that glycan-glycan interaction is Ca^{2+}-dependent and that increase in Ca^{2+} concentration leads to the enhancement in adhesive forces. We propose that these outermost cell surface structures serve as important players initiating the first contacts between cells through flexible but nevertheless specific carbohydrate-carbohydrate chain interactions.

Materials and methods

Sponges, live cells, cell surface proteoglycans and glycans

Microciona prolifera, Halichondria panicea, Suberites fuscus and *Cliona celata* were collected at the Marine Biological Laboratory Marine Resources Department in Woods Hole, Mass. Live sponge cells were isolated as described previously [26]. Isolation of cell surface proteoglycans and pronase digestion of 200-kDa glycans from core structures were carried out as described [24,30]. Only freshly prepared cells and glycans were used for all experiments and analyses.

Analytical methods

For carbohydrate composition, proteoglycans were hydrolyzed in 4 M TFA at 100°C for 4 h and the remaining TFA removed by methanol-aided evaporation. Carbohydrates were analyzed by high performance anion exchange chromatography using a Dionex BioLC system and a CarboPac PA1 column. The column was equilibrated with 16 mM NaOH and eluted with linear gradients of 16 mM NaOH to 0.1 M NaOH/50 mM Na-acetate or to 0.1 M NaOH/180 mM Na-acetate. Pulsed amperometric detection was carried out using PAD 2 cells with E1 = +0.05 V, 480 ms, E2 = +0.75 V, 180 ms, and E3 = −0.20 V, 360 ms. Relative amounts were calculated using relative response factors from standard samples containing 2 nM of the respective monosaccharides treated in the same way as the polysaccharide samples.

Amino acid analyses were performed as described [3]. Briefly, dry glycan samples were hydrolyzed for 24 h and the black residues were suspended in 100 μl of 50 mM HCl containing 50 pM/μl Sar and Nva. After centrifugation, the transparent solutions were transferred into new reagent tubes and analyzed with a Hewlett-Packard AminoQuant II analyzer.

Long term EDTA-treatment of sponge proteoglycans

2 ml of 0.7 mM EDTA, pH 7.0 was added to lyophilized proteoglycans, and left at 4°C for a 4-week period. Following this treatment, separation of the core structures and the arms was achieved on A-15m BioRad column (1.5 × 90 cm), eluted with 0.5 M NaCl, 10 mM Tris, pH 7.4. Collected fractions were lyophilized.

Aggregation assays

Freshly sonicated fluorescent carboxylate-modified beads (3.6×10^8) (Molecular Probes, 1 μm diameter) were incubated overnight at room temperature, pH 6.0, with 200-kDa glycans (1.5 mg/ml) in Ca^{2+}- and Mg^{2+}-free artificial seawater buffered with 20 mM Tris pH 7.4 supplemented with 2 mM $CaCl_2$(CSW), 3 mg water-soluble 1-ethyl-3-(3 dimethylaminopropyl) carbodiimide (EDAC, Molecular Probes), and 1 mg N-hydroxysulfosuccinimide (Molecular Probes). Coupling efficiency was determined by dotting a bead aliquot on a Zeta probe membrane and Alcian Blue staining. The density of 200-kDa glycan molecules on the bead surface was calculated from the specific absorbance of stained glycans, which gave the number of moles (0.15×10^{-11}), Avogadro's number (6.022×10^{23}) and the number of beads (3.6×10^8).

Glycan-coated red amine-modified beads (9×10^6) [3] in 400 μl of CSW were allowed to aggregate with cells, and glycan-coated carboxylate-modified beads (3.6×10^8) in 400 μl of CSW were allowed to aggregate with other glycan-coated carboxylate-modified beads on a rotary shaker at 50 rpm for 4 h after the addition of 10 mM $CaCl_2$. Images of aggregates were acquired with a confocal laser-scanning microscope (Leica Lasertechnik, Heidelberg, Germany) equipped with an argon/krypton laser and a ×10 objective (PL Fluotar, N.A. 0.3). Image processing was performed using Adobe Photoshop version 6.0. Data were quantified using UTHSCSA Image Tool version 2.00 Alpha.

Binding of cells and glycans to glycan-coated plates

Solid phase polystyrene plastic surfaces coated with 200-kDa glycans were prepared as described [3]. Binding of cells to glycan-coated plates was done as before [3]. Briefly, 100 μl of live cells (5×10^3) in CSW were added to each glycan-coated well and incubated for 2 h at room temperature after addition of 200 μl of CSW containing 10 mM $CaCl_2$. Afterwards, non-adherent cells were washed off with CSW containing 10 mM $CaCl_2$. Bound cells were lysed for 10 min in 2M NaCl, 20 mM Tris-HCl, pH 7.5. Hoechst stain (200 ng) in 20 mM Tris-HCl, pH 7.5 was added to cell lysates and the fluorescence measured at $\lambda_{ex} = 360$ nm and $\lambda_{em} = 450$ nm. Glycans (100 μl) in CSW (0.1 mg/ml) were added to glycan-coated plates and incubated for 2 h at room temperature after addition of 10 mM $CaCl_2$. Afterwards, non-bound glycans were washed off with CSW containing 10 mM $CaCl_2$. Bound glycans were stained with 1% Toluidine Blue and absorbance measured at 630 nm. The absorbance of glycans used as a coat was deducted from the total absorbance of glycans coated on wells and glycans bound to glycan-coated plates to give the final absorbance of bound glycans.

Atomic force microscopy

Force measurements were performed as before [3] with a commercial Nanoscope III AFM (from Digital Instruments, Santa Barbara, Calif., USA) equipped with a 162-μm scanner (J-scanner) and oxide-sharpened Si_3N_4 cantilevers with a thickness of 400 nm and a length of 100 μm. Measurements of cantilever spring constants for a series of cantilevers from the same region of the wafer gave an average of $k = 0.085$ N/m and a standard deviation of 0.002 [31]. All measurements were done with cantilevers from the same batch. AFM supports were built as described [32]. Gold (20 nm) was deposited on the mica surface and the tip using a pressure of 5×10^{-2} mbar controlled by a quartz thickness and deposition rate monitor (Bal-Tec QSG 050).

Gold coated Si_3N_4 tips and micas allowed covalent chemisorptions of the naturally sulfated carbohydrates. The support and the tip were incubated with 200-kDa glycans (1 mg/ml) in CSW for 15 min at room temperature. Non-bound glycans were washed off with CSW and glycan-glycan force measurements performed in CSW containing 10 mM or 100 mM $CaCl_2$. For each measurement, a new tip was coated with 200-kDa glycan and a new Au substrate was prepared. The AFM stylus approached and retracted from the surface approximately 100 times with a speed of 200 nm/s. The tip was moved laterally 50 nm after recording five force-distance curves.

Surface clustering of 200-kDa glycans on the support and on the tip was determined by fluorescence imaging of bound

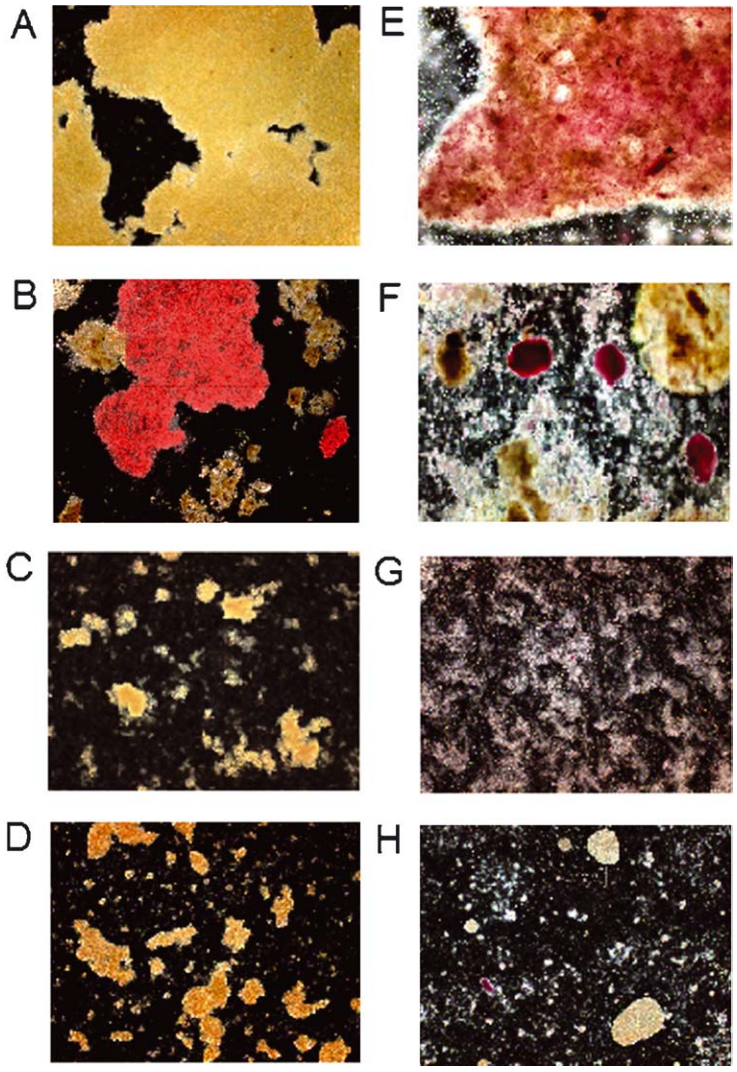

Figure 1.

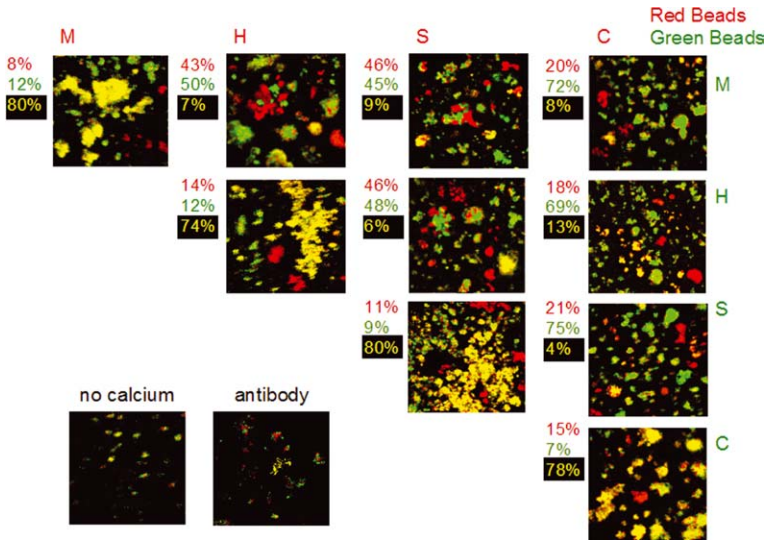

Figure 2.

glycans labeled at the amino groups of the amino acid portion with 5(6)-carboxyfluorescein-N-hydroxysuccinimidester (Boehringer Mannheim).

Results

Species-specific aggregation between live cells and between cells and cell surface glycan coated on beads

Mechanically dissociated sponge cells sort out and reaggregate species-specifically in artificial seawater at physiological Ca^{2+} concentrations (10 mM) under carefully controlled shear forces, *i.e.* rotor speed. Too high rotation causes cell aggregates to come apart and too low rotation leads to formation of unspecific, faulty aggregates between cells that do not get a second or third chance to form higher affinity adhesions with other cells. When live cells from the same species were shaken in suspension at the right shear forces, they formed large homogenous aggregates (Figure 1A). However, cells from two different species sorted out into separate aggregates consisting only of cells from the same species (Figure 1B). This specific cell-cell recognition was drastically reduced in the absence of Ca^{2+} in the artificial seawater (Figure 1C). A monoclonal antibody directed against the carbohydrate epitope of *Microciona* cell surface proteoglycan reduced the aggregation of *Microciona* cells only (Figure 1D).

Red beads similar in size to small sponge cells were coated with 200-kDa glycans isolated from the core structures of different proteoglycans. Glycan-coated beads were allowed to aggregate with live cells under the conditions used for cell-cell aggregation. Cells specifically recognized beads coated with their own surface glycans (Figure 1E). However, they did not mix but formed separate aggregates with beads coated with glycans from different species (Figure 1F). The absence of Ca^{2+} reduced this species-specific cell-glycan recognition (Figure 1G). The monoclonal antibody against the carbohydrate epitope of *Microciona* proteoglycan reduced only the recognition between *Microciona* cells and beads coated with their glycan (Figure 1H).

Species-specific aggregation between glycan-coated beads mimicking species-specific cell-cell aggregation

It has been shown recently that amine-modified beads coated with 200-kDa glycans from different species can aggregate species-specifically in the same way as live cells [3]. A further type of bead, carboxylate-modified beads that require different method for coupling of glycans, was coated with different 200-kDa glycans and examined for aggregation under the conditions used previously for cell-cell and cell-glycan recognition. Beads coated with glycans from identical proteoglycans formed 80% to 74% yellow aggregates, which are the result of the intermingling of red and green beads (Figure 2). In stark contrast, beads coated with glycans derived from proteoglycans of different species separated into red and green aggregates. In this case, yellow aggregates, *i.e.* heterotypic mixtures of glycans originating from different species, formed only 4% to 13% of patches. As shown previously for cell-cell and cell-glycan recognition, the absence of Ca^{2+}-ions inhibited glycan-glycan recognition (Figure 2). The monoclonal antibody against the carbohydrate epitope of the *Microciona* proteoglycan inhibited only the homotypic interaction between *Microciona* glycans coated on red and green beads (Figure 2).

It has been reported previously that 400 molecules of *Microciona* proteoglycan bound per cell caused live cells to aggregate [26]. As one proteoglycan carries ~26 copies of 200-kDa glycan, ~10'400 glycan molecules per cell cause living cells to aggregate. In our studies, binding measurements indicated that

Figure 1. Specific recognition between live cells (A–D), and between cells and glycans (E–H). A, Yellow cells from the same species (*Suberites fuscus*) formed large homogenous aggregate during a 4-h rotation-mediated aggregation in artificial seawater with physiological 10 mM $CaCl_2$. B, Cells from two different species, with red (*Microciona prolifera*) and grey (*Halichondria panicea*) natural pigments, form separated bright red and grey aggregates. C, Absence of Ca^{2+} inhibited cell-cell aggregation (aggregation between *Halichondria* and *Suberites* cells as an example). D, The monoclonal antibody directed against the carbohydrate epitope of *Microciona* proteoglycan reduced aggregation between *Microciona* cells (40 μg of the antibody with 5×10^3 cells). E, Grey cells (*Halichondria*) formed one big aggregate with their own surface glycans coated on red beads. F, Grey cells (*Halichondria*) formed their own aggregates separated from red aggregates of beads carrying glycans from another species. G, The absence of Ca^{2+} reduced cell-glycan aggregation (aggregation between *Halichondria* cells and *Microciona*-coated beads as an example). H, The monoclonal antibody directed against the carbohydrate epitope of *Microciona* proteoglycan reduced aggregation between *Microciona* cells and their glycan coated on beads (40 μg of the antibody with 4.5×10^8 glycan-coated beads).

Figure 2. Specific recognition between glycan-coated beads. Glycan-coated carboxylate-modified beads sorted out specifically during a 4-h rotation-mediated aggregation in artificial seawater with physiological 10 mM $CaCl_2$. The numbers on the left side of each picture represent the percentage clumps of the respective color. Yellow areas depict aggregates of mixed red and green beads coated with identical glycans. Red and green areas reflect aggregates of separated beads coated with different glycans. The absence of Ca^{2+} in artificial seawater inhibited glycan-coated bead-bead aggregation. The monoclonal antibody directed against the carbohydrate epitope of *Microciona* proteoglycan inhibited aggregation between *Microciona* glycans coated on beads (40 μg of the antibody with 9×10^6 glycan-coated beads). M,*Microciona*; H, *Halichondria*; S, *Suberites*; C,*Cliona*.

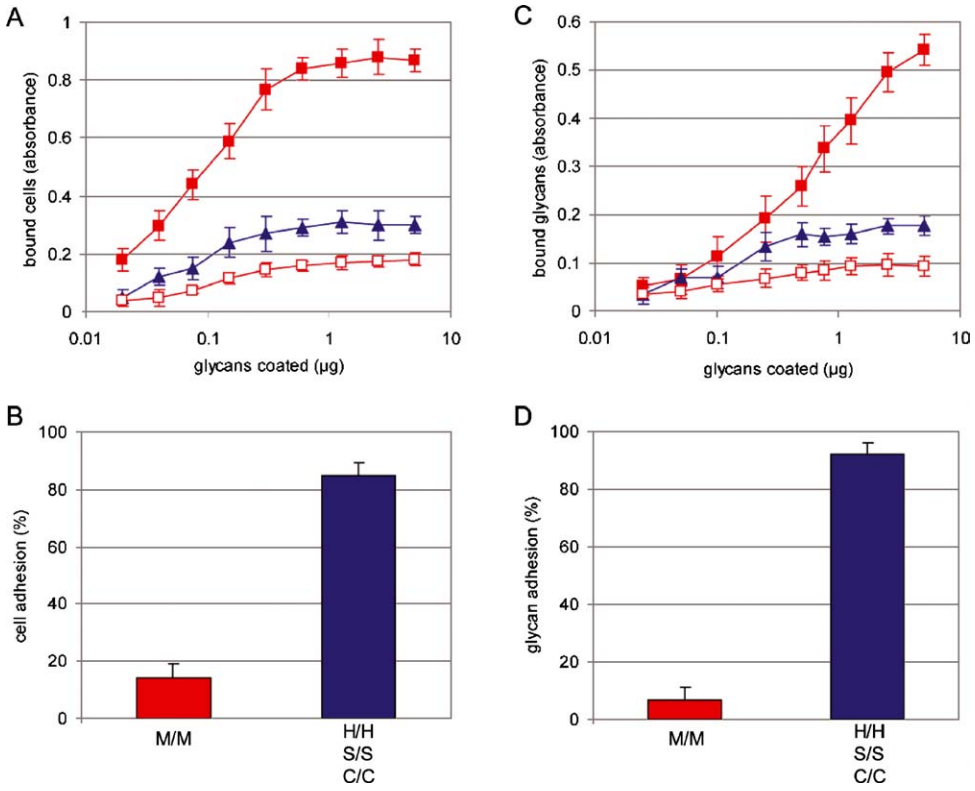

Figure 3.

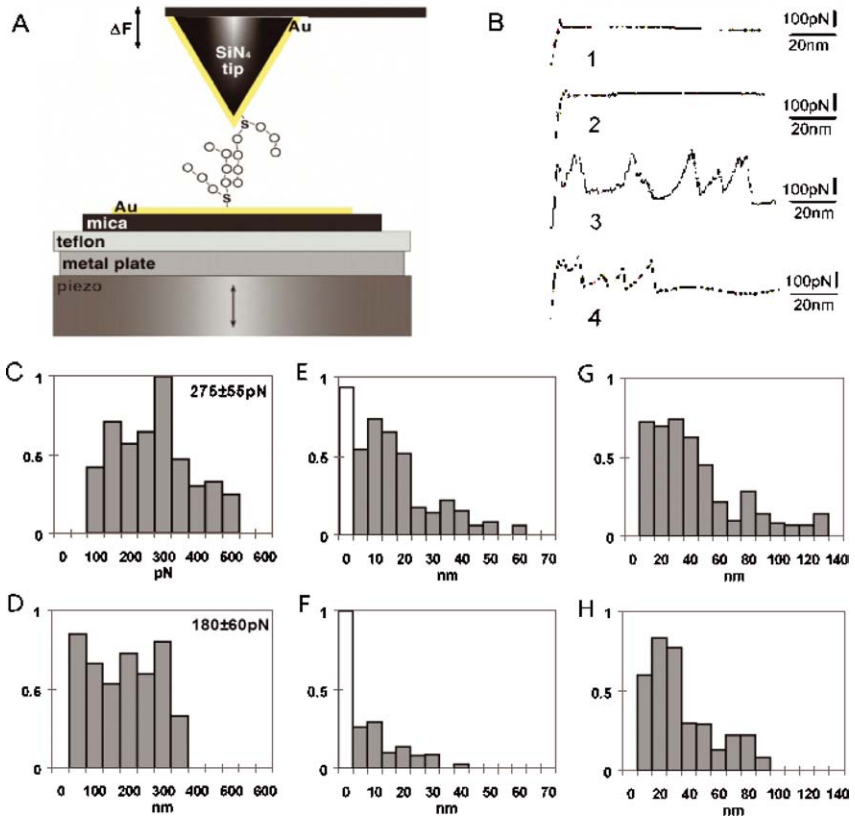

Figure 4.

~2500 molecules of 200-kDa glycan per bead specifically aggregated glycan-coated carboxylate-modified beads. This was calculated from the number of moles and Avogadro's number, divided by the number of beads (see Materials and Methods). Surface areas of cells and beads were calculated from their diameters. Thus, the glycan densities causing species-specific live cell and glycan-coated bead recognition and aggregation are similar: 828 molecules/μm^2 for cell-cell aggregation and 800 molecules/μm^2 for glycan-coated bead-bead aggregation.

Species-specific adhesion of live cells and cell surface glycans to glycans coated on plastic surfaces

Plastic surfaces were coated with 200-kDa glycans from four different species of surface proteoglycans. Mechanically dissociated cells were added to wells and the ability and specificity of live sponge cells to adhere to different glycans coated onto a solid phase were studied. Live cells strongly adhered to glycans from their own surface proteoglycans in the presence of physiological 10 mM Ca^{2+}-ions in artificial seawater. The binding of cells to glycans from different species of proteoglycans was 4- to 4.5-fold lower (Figure 3A). This species-specific cell-glycan adhesion was clearly dependent on the amount of the glycan coated and was almost completely abolished in the absence of Ca^{2+}. Pretreatment of cells with a monoclonal antibody directed against the carbohydrate epitope of *Microciona* proteoglycan inhibited homotypic interactions between *Microciona* cells and their own glycan coated on the surface (Figure 3B). Only little cross-reactivity of the antibody was detected and it blocked 12% of the homotypic interactions between cells from three other studied species and their glycans.

Similarly, the ability of glycans isolated from the core structures of different sponge proteoglycans to adhere to glycan-coated surfaces was studied. Glycans mimicked live cells and only adhered strongly to surface-bound glycans from the same species proteoglycan (Figure 3C). They adhered 3.5- to 4-fold less to glycans from different species proteoglycans. As in the adhesion of live cells to glycan-coated surfaces, the glycan-glycan adhesion was also dependent on the amount of the glycan coated and was abolished in the absence of Ca^{2+}. Pretreatment of glycans with a monoclonal antibody directed against the carbohydrate epitope of *Microciona* proteoglycan inhibited only homotypic *Microciona* glycan-glycan

Figure 3. Specific adhesion of live cells and glycans to glycan-coated plates. A, Cells adhered species-specifically to 200-kDa glycans from core structures of different sponge proteoglycans coated on plastic plates. (■), Homotypic adhesion of live cells to their own glycans coated on plates (average from experiments where live cells from 4 different sponge species: *Microciona prolifera*, *Halichondria panicea*, *Suberites fuscus*, and *Cliona celata* were tested for binding to their own glycans coated on plates); (▲), Heterotypic adhesion of live cells to different glycans coated on plates (average of experiments where live cells from 4 different sponge species were tested for binding to glycans from species different from their own) ; (□), Adhesion of live cells from 4 different species to their own glycans without the presence of Ca^{2+}. B, Effect of the monoclonal antibody directed against the carbohydrate epitope of *Microciona* proteoglycan on homotypic adhesion between *Microciona* cells and *Microciona* glycan coated on plates (40 μg of the antibody with 5×10^3 cells). C, Glycans adhered species-specifically to glycan-coated plastic plates. (■), Homotypic adhesion of 200-kDa glycans to the same glycans coated on plates (average from experiments where glycans from 4 different sponge species: *Microciona*, *Halichondria*, *Suberites*, and *Cliona* were tested for binding to the same glycans coated on plates); (▲), Heterotypic adhesion of 200-kDa glycans to different glycans coated on plates (average of experiments where glycans from 4 different sponge species were tested for binding to glycans from species different from their own); (□), Adhesion of glycans from 4 different species to the same glycans coated on plates without the presence of Ca^{2+}. D, Effect of the monoclonal antibody directed against the carbohydrate epitope of *Microciona* proteoglycan on homotypic adhesion between *Microciona* glycans (40 μg of the antibody with 10 μg of glycans). M/M, *Microciona-Microciona* adhesion; H/H, *Halichondria-Halichondria* adhesion; S/S, *Suberites-Suberites* adhesion; C/C, *Cliona-Cliona* adhesion. $\pm$ SD from 16 independent experiments.

Figure 4. Atomic Force Microscopy (AFM) measurements of glycan-glycan binding forces. A, Scheme of AFM set-up for the measurement of the intermolecular forces between single glycan molecules. B, Examples of AFM force curves. Line 1 and 2 represent control curves: gold-gold interaction (1) and homotypic glycan-glycan interaction in artificial seawater without Ca^{2+} (2). Line 3 represents a curve of the homotypic interaction between glycans from the same species, and line 4 the heterotypic interaction between glycans from two different species in the presence of physiological 10 mM Ca^{2+}. C, Adhesion force values of the homotypic interactions between glycans from the same species attached to the tip and the mica surface (average from homotypic binding experiments between glycans from 4 sponge species: *Microciona prolifera*, *Halichondria panicea*, *Suberites fuscus*, and *Cliona celata*). D, Adhesion force values of the heterotypic interactions between glycans from different species (average from heterotypic binding experiments between glycans from 4 different sponge species). E, Periodicity measurements showing distances between individual rupture peaks, which indicate the distances between binding motifs on the carbohydrate chain for homotypic interactions between the same species glycans and F, for heterotypic interactions between glycans from different species. The white bar reflects the number of probe lift events where only one rupture event was registered. G, The length of the force curves measured from the lift-off point to the last peak, indicating the total length of the interacting carbohydrate chain between the same species glycans and H, between different species glycans. On the ordinate, the number of rupture events is provided normalized to 1.0 for the category of the highest number of events.

adhesion (Figure 3D). The antibody blocked only 6% of the homotypic glycan-glycan adhesion between other sponge species.

AFM measurements of the carbohydrate-carbohydrate interaction

AFM has the precision and sensitivity necessary for studying molecular recognition under native conditions at the level of single events at forces in the pN range. An AFM tip and a surface were coated with 200-kDa glycan molecules from different sponge species (Figure 4A) [3]. There were no multilayers or clusters of glycans on the tip or the surface. Intermolecular adhesion force measurements between single glycan molecules were performed in artificial seawater with physiological 10 mM Ca^{2+}. During retraction of the tip, the glycan structure was lifted and stretched and non-covalent bonds between two molecules were eventually broken one by one. The existence of multiple non-covalent bonds between carbohydrates of glycan molecules was suggested by the presence of multiple peaks on force curves, as recorded in the presence of Ca^{2+} (Figure 4B, line 3).

Monitored cantilever deflection is a direct measure of the forces between interacting glycan molecules. No interaction was recorded between gold-gold (Figure 4B, line 1), in the absence of Ca^{2+}(line 2) or during the surface approach. On retraction, the sensor tip detected strong multiple interactions between 200-kDa glycans from the same species (Figure 4B, line 3). Clearly reduced interactions were detected between glycans from two different species (Figure 4B, line 4). Binding forces between glycans from the same species were on average 275 pN (Figure 4C), compared with binding forces between glycans from different species of 180 pN (Figure 4D). A statistical analysis using the Mann-Whitney test (P values clearly below 0.01) showed the difference to be significant.

The interactions between single 200-kDa glycans were polyvalent, *i.e.* interactive sites were repeated along the carbohydrate chain; this is suggested by the presence of multiple peaks on force curves. The distance between peak numbers 1 and 2 (2 and 3, etc.) was measured to produce a histogram of the peak periodicity (Figure 4E and F). Force curves representing interactions between two single glycan molecules from the same species showed convincing multiple interaction peaks. Over 80% of force curves representing interactions between glycans from the same species showed more than one interaction peak, with a distance between binding motifs of 10–20 nm. In contrast, only ∼25% of force curves between glycans from different species showed multiple interaction peaks, demonstrating a preference for one rather unspecific binding event during the interaction.

Interaction sites for glycans from the same species were located along the carbohydrate chain and not only at its end. The total lengths of most force curves did not exceed 50 nm (∼75%), though in some cases the curves extended up to 130 nm (Figure 4G). In contrast, force curves for the glycans from different species showed less extensions and almost 80% of the total lengths were only 10–40 nm (Figure 4H).

Enhancement of the strength of the carbohydrate-carbohydrate interaction by increasing Ca^{2+}

The role of Ca^{2+}-ions in carbohydrate-carbohydrate interactions was studied by increasing the Ca^{2+}concentration in artificial seawater from physiological 10 mM to 100 mM during AFM measurements of the adhesion forces between single *Microciona prolifera* 200-kDa glycans. A single non-covalent bond between two interacting *Microciona* glycan molecules was ruptured at 310 pN in 10 mM Ca^{2+} (Figure 5B). This adhesion force increased to 375 pN when the Ca^{2+} concentration was increased to 100 mM (Figure 5F). A statistical analysis revealed P values clearly below 0.01 and, therefore, showed the difference between these two interactions to be significant.

The occurrence of polyvalent interactions between single glycan molecules was higher in 100 than in 10 mM Ca^{2+}. In 100 mM Ca^{2+}, up to 85% of force curves showed the presence of multiple interaction sites with a distance between binding motifs of 10–20 nm (Figure 5G). In 10 mM Ca^{2+}, ∼70% of force curves also showed multiple peaks, indicating repetition of binding sites along the interacting carbohydrate chain of the glycan molecule (Figure 5C).

The total lengths of interacting carbohydrate chains did not change with the change in Ca^{2+} concentration. In both cases, the greatest extensions of the interacting carbohydrate chain were up to 120 nm (Figure 5D and H). The total lengths of force curves were mainly 20–50 nm in 10 and in 100 mM Ca^{2+}. However, longer force curves, *i.e.* longer interacting carbohydrate chains, were more frequent for glycan-glycan interaction in 100 than in 10 mM Ca^{2+}. Up to 13% of force curves were more than 80 nm long in 100 mM Ca^{2+} (Figure 5H) compared with only ∼3% in 10 mM Ca^{2+} (Figure 5D).

Species-specific carbohydrate composition of proteoglycan molecules from different species

Proteoglycan molecules from four different sponge species were subjected to EDTA-treatment to separate the core structures from the arms (Figure 6A). Extensive pronase digestion of purified core structures led to essentially pure 200-kDa glycan fractions, which mediate cell-cell recognition through self-interactions, and pronase digestion of purified arms gave pure 6-kDa glycan fractions, which mediate binding of the proteoglycan to the cell surface (Figure 6B). 200-kDa glycans were free of protein contamination (Table 1). There was essentially no loss of carbohydrates during the purification procedures (carbohydrate yield ∼97%). Amino acid analysis of purified glycans showed 0.7 (*Cliona celata*) to 1.1 (*Microciona prolifera*) mol of linker aspartate per mol glycan. Only trace amounts of a few other amino acids were detected. We are aware that aspartate is not a classical linker amino acid in proteoglycans,

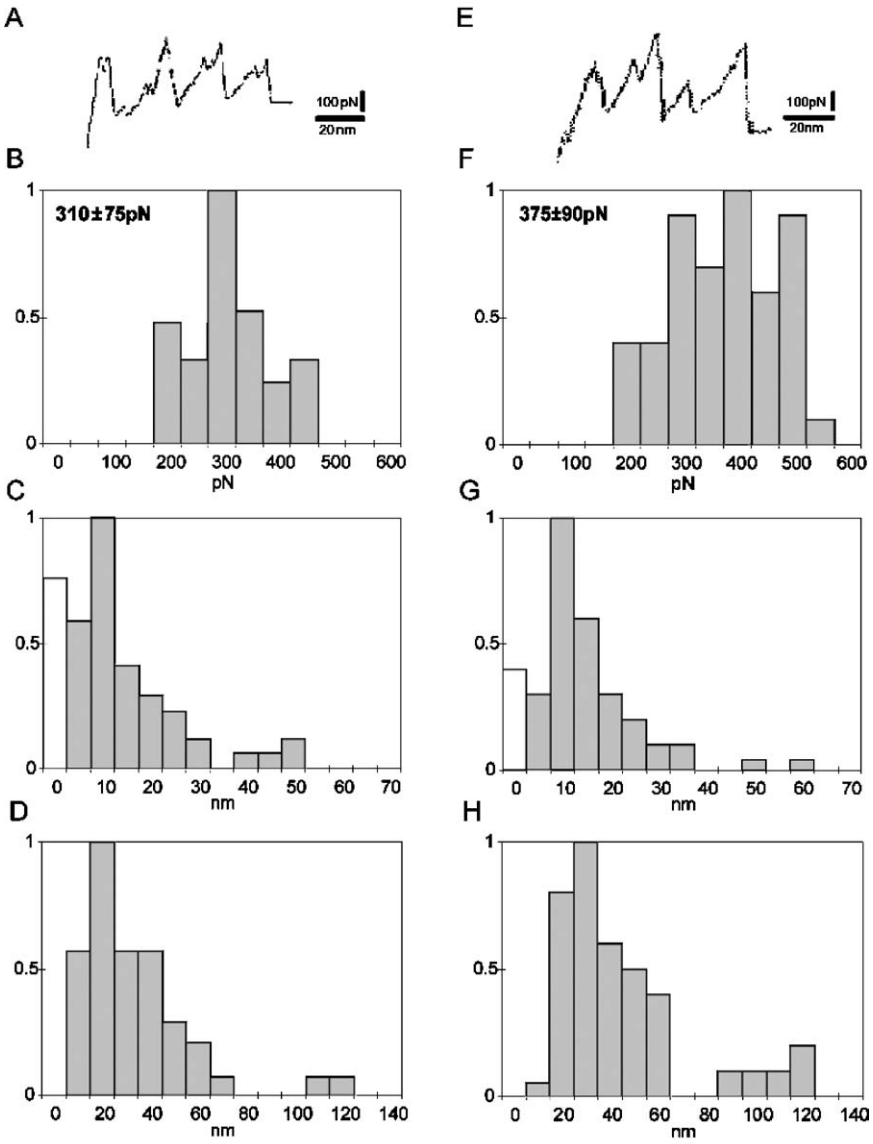

Figure 5. Quantitative evaluation of interactions between single glycan molecules in physiological 10 mM Ca^{2+} (A–D) versus interactions in 100 mM Ca^{2+} (E–H). Interactions between *Microciona prolifera* glycans were measured in artificial seawater with 10 and 100 mM Ca^{2+}. A, An example of AFM force curve of the glycan-glycan interaction in 10 mM Ca^{2+}. B, Adhesion force values for glycan-glycan interactions in 10 mM Ca^{2+}. C, Periodicity measurements of distances between rupture peaks, which indicate the distances between binding motifs on the carbohydrate chain, in 10 mM Ca^{2+}. D, The total length of the interacting carbohydrate chain in glycan-glycan interactions in 10 mM Ca^{2+}. E, An example of AFM force curve of the glycan-glycan interaction in 100 mM Ca^{2+}. F, Adhesion force values for glycan-glycan interactions in 100 mM Ca^{2+} and H, 100 mM Ca^{2+}.G, Periodicity measurements of distances between rupture peaks in 100 mM Ca^{2+}. H, The total length of the interacting carbohydrate chain in glycan-glycan interactions in 100 mM Ca^{2+}.

but the EM morphology and size of these sponge glycoconjugate molecules are similar to the mammalian proteoglycans. Its sulfate and glucoronate content and cellular location led to the term sponge proteoglycans 30 years ago and we prefer, until a detailed structure is known, to stay with this terminology.

The carbohydrate compositions of purified proteoglycans from four different sponge species were analyzed by high performance anion exchange chromatography. All proteoglycans contained galactose (Gal), fucose (Fuc), mannose (Man), *N*-acetylglucosamine (GlcNAc), N-acetylgalactosamine (GalNAc), and glucuronic acid (GlcUA). The carbohydrate makeup of proteoglycans from different individuals of the same species was very similar, while proteoglycans from different species showed large differences (Table 2). *Microciona* proteoglycan was characterized by high fucose, while *Halichondria* proteoglycan had 3-fold less. *Microciona* and

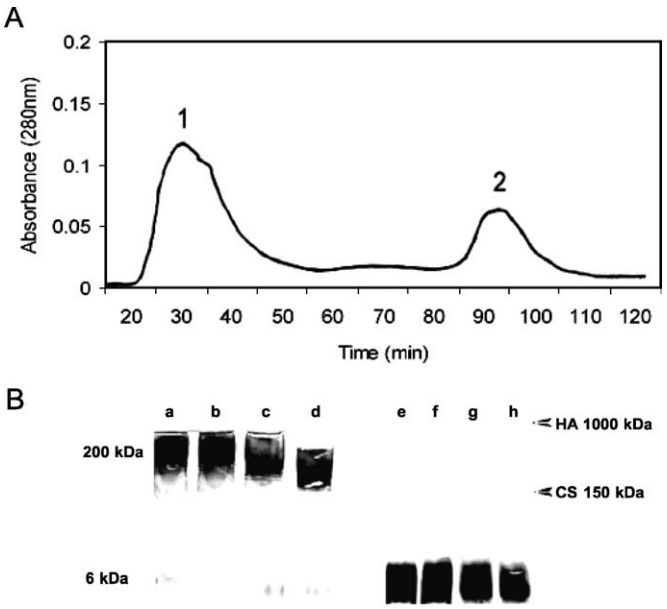

Figure 6. Separation of glycans obtained by pronase digestion of core structures and arms of different sponge proteoglycans. A, Separation of two proteoglycan subunits on A-15m sizing column after prolonged EDTA-treatment of proteoglycan molecules (an example of separation of *Microciona prolifera* proteoglycan subunits; peak nr 1: core structures of the proteoglycan, peak nr 2: arm fragments of the proteoglycan). B, PAGE electrophoresis of glycans obtained by pronase digestion of two subunits. a–d, 200-kDa glycans from 4 different sponge species obtained from the peak nr 1; e–h, 6-kDa glycans from 4 different species obtained from the peak nr 2. a and e, *Microciona prolifera* glycans; b and f, *Halichondria panicea* glycans; c and g, *Suberites fuscus* glycans; d and h, *Cliona celata* glycans. Molecular weight standards: HA, hyaluronic acid; CS, chondroitin sulfate.

Halichondria proteoglycans showed high galactose, while *Cliona* proteoglycans had 3- to 4-fold less. The latter was the only species with significant amounts of GalNAc. On the other hand, only *Microciona* proteoglycan contained significant amounts of GlcUA.

Discussion

Until recently, specific proteoglycan-mediated cell adhesion and recognition processes could not be assigned to glycan-glycan recognition. This report presents comparative data on species-specificity and strength of self-interactions between glycans derived from cell surface proteoglycans. The glycan-glycan interaction is characterized by binding forces in the range of 200–300 pN, by species-specificity, polyvalency, and is stabilized by Ca^{2+}-ions.

Adhesive forces measured between glycans from the same species (275 pN) are the strongest forces reported to date for direct carbohydrate-carbohydrate interactions [3]. They are as strong as forces measured for the proteoglycan-proteoglycan interaction (50–400 pN) [33] as well as those for single antibody-antigen recognition (244 pN) [34,35]. These observations support the notion that direct carbohydrate-carbohydrate interaction is strong enough to manifest itself in biologically relevant cellular recognition. However, even lower values of adhesion forces, *e.g.* the adhesion force for glycosphingolipid self-interactions in the interactions between $Lewis^x$ structures (20 pN) [36], cannot exclude biological relevance. Carbohydrate molecules offer the multivalent presence of oligosaccharide chains on cell surfaces that could easily enhance weak binding forces and affinities to the levels found in biologically relevant interactions [37].

Table 1. Trace amino acid composition of 200 kDa glycans from four sponge species. The values are the average of four determinations. Cys was not determined

	Microciona	*Halichondria*	*Suberites*	*Cliona*
	(mol amino acid/mol glycan)			
Asp	1.1	0.9	0.9	0.7
Glu	0.4	0.3	0.4	0.2
Ser	0.2	0.1	0.2	0
His	0	0	0	0
Gly	0.3	0.3	0.2	0.3
Thr	0.4	0.1	0	0.1
Ala	0.2	0.1	0.1	0
Arg	0	0	0	0
Tyr	0	0	0	0
Val	0	0	0	0
Met	0	0	0	0
Phe	0	0.1	0	0
Ile	0	0	0	0
Leu	0	0.1	0.1	0
Lys	0	0	0	0
Pro	0	0	0	0
Asn	0	0	0	0
Gln	0	0	0	0
Trp	0	0	0	0
Ca	0	0	0	0
Total	2.6	2.0	1.9	1.3

Table 2. Comparison of the carbohydrate composition of proteoglycans from four sponge species. The average values were obtained from four sponge individuals of each species

	Microciona	*Halichondria*	*Suberites*	*Cliona*
	(carbohydrates (mol%))			
Fuc	30.2	8.2	15.0	22.1
Gal	33.5	40.9	25.0	10.8
Man	9.7	15.2	12.4	14.0
GalNAc	3.7	1.2	2.0	10.1
GlcNAc	18.3	14.1	34.2	27.5
GlcUA	9.1	3.0	1.9	4.5

The species-specificity of glycan-mediated recognition is guaranteed not only by the greater adhesion forces but also by higher frequency of polyvalency in interactions between identical glycans versus different glycans, by differences in carbohydrate composition, and probably by the arrangement of glycan chains in a three-dimensional context. Polyvalency, *i.e*. the repetition of interactive sites along the carbohydrate chain, can generate sufficient affinity and/or avidity for carbohydrates to function in biologically relevant recognition events. A suitable mechanism for keeping two interacting carbohydrate chains arranged in a polyvalent array would be a zipper. This model provides both the simplicity and driving force by which nature may create specificity between two compositionally rather similar structures interacting with one another [38]. Polyvalent glycans on cell surfaces, therefore, represent a highly flexible and specific model for a recognition system that allows cells to test surrounding surfaces and first create weak, random contacts before releasing or reinforcing the adhesion.

Differences in carbohydrate composition and the arrangement of a glycan chain in a three-dimensional context can also define the specificity of the carbohydrate-carbohydrate interaction. The carbohydrate composition (Fuc, Gal, Man, GalNAc, GlcNAc, and GlcUA) is highly conserved between individuals of the same species, whereas large differences are seen between different species. Detailed structural analyses of different proteoglycans have revealed species-specific sequences [39]. Diversity of polysaccharide primary structure affords diversity in higher order structure, and the specificity of the carbohydrate-carbohydrate interaction may be provided also by the three dimensional spatial relationships of the sugars.

Ca^{2+}-ions or other divalent cations are crucial in carbohydrate-carbohydrate interaction. In marine sponges they are essential. At the molecular level, Ca^{2+} probably reinforces the contact between the interacting oligosaccharides of glycan molecules, since an increase in Ca^{2+} in the buffer led to an increase in adhesion forces and in polyvalent interactions. In measurements of adhesion forces between sulfated disaccharides, it was also reported that Ca^{2+} probably provides coordinating forces [29]. However, the presence of Ca^{2+}-ions did not contribute significantly to the adhesion force in Le^x-Le^x interactions measured by AFM [36]. There is also no Ca^{2+} in the Le^x crystal [40]. Therefore, it was implied that calcium is only responsible for the approach and organization of the carbohydrates in the cell membrane. In contrast, corneal epithelial cell-cell adhesion through the Le^x determinant turned out to be highly dependent on the presence of Ca^{2+}-ions [41]. Similarly, self-aggregation of Le^x molecules in aqueous solution, where the molecules move freely, occurs only in the presence of Ca^{2+}-ions [42].

Rare ionic interactions cannot be excluded as most carbohydrates are neutral or negatively charged due to carboxy- and sulfate-groups, and even positively charged glycans also occur. However, the Ca^{2+} effect is not merely a charge effect. It has been shown that acidic sponge glycans do not all interact in the presence of Ca^{2+} [43]. Although single hydroxyl groups are too weak to coordinate cations, the combination of just two well-positioned hydroxyl groups on one sugar residue or over two neighboring residues can lead to coordinate bonds between two interacting carbohydrate chains in the presence of water molecules. These Ca^{2+} interactions together with hydrogen bonds may lead to a sort of super-structure which then could bring about and allow even internal lipophilic interactions [1].

The role of Ca^{2+} in carbohydrate-carbohydrate interactions is still not well understood. Ca^{2+}-ions could be responsible for the approach and organization of the sugar moieties providing the surfaces for interaction, or they could enhance directly the adhesion force between complementary surfaces, acting as a bridge between specific hydroxy groups. Further experimental contributions to these potential models are now required before any of these proposals could be considered as relevant, in particular biologically relevant.

Better methods for the synthesis and characterization of carbohydrates are creating numerous opportunities for elucidation of the biological roles of these outermost cell surface structures. Carbohydrate-carbohydrate recognition is only one of the many possible oligosaccharide interactions for which a molecular level understanding is deficient or lacking completely. If carbohydrate-carbohydrate interactions may ensure adequate cell behavior during the formation, maintenance, and pathogenesis of tissues, a thorough understanding of the chemical and molecular nature of specific carbohydrate-carbohydrate recognition will be a prerequisite for the development of strategies to modify it and to progress thereby in an understanding of its biological relevance.

Acknowledgments

We thank S. Scheuring and A. Engel for collaboration on AFM, and S. Hakomori for providing the technical training required for experiments involving binding to coated plates. This work was supported by the Friedrich Miescher Institute, which is a branch of the Novartis Research Foundation, as well as the M. E. Müller Foundation and the Swiss National Research Foundation.

References

1 Spillmann D, Burger MM, Carbohydrate-carbohydrate interactions in adhesion, *J Cell Biochem* **61**, 562–8 (1996).
2 Varki A, Selectin ligands, *Proc Natl Acad Sci USA* **91**, 7390–7 (1994).
3 Bucior I, Scheuring S, Engel A, Burger MM, Carbohydrate-carbohydrate interaction provides adhesion force and specificity for cellular recognition, *J Cell Biol* **165**, 529–37 (2004).
4 Nakano M, Kakehi K, Tsai MH, Lee YC, Detailed structural features of glycan chains derived from {alpha}1-acid glycoproteins of several different animals-The presence of hypersialylated, O-acetylated sialic acids but not disialy residues, *Glycobiology* **14**, 431–44 (2004).

5 Bush CA, Martin-Pastor M, Imberty A, Structure and conformation of complex carbohydrates of glycoproteins, glycolipids, and bacterial polysaccharides, *Annu Rev Biophys Biomol Struct* **28**, 269–93 (1999).

6 Berninsone PM, Hirschberg CB, The nematode Caenorhabditis elegans as a model to study the roles of proteoglycans, *Glycoconj J* **19**, 325–30 (2002).

7 Hakomori S, Structure, organization, and function of glycosphingolipids in membrane, *Curr Opin Hematol* **10**, 16–24 (2003).

8 Hakomori S, Handa K, Glycosphingolipid-dependent cross-talk between glycosynapses interfacing tumor cells with their host cells: Essential basis to define tumor malignancy, *FEBS Letters* **531**, 88–92 (2002).

9 Kasahara K, Sanai Y, Functional roles of glycosphingolipids in signal transduction via lipid rafts, *Glycoconj J* **17**, 153–62 (2000).

10 Hakomori S, Cell adhesion/recognition and signal transduction through glycosphingolipid microdomain, *Glycocon J* **17**, 143–51 (2000).

11 Fenderson BA, Zehavi U, Hakomori S, A multivalent lacto-N-fucopentaose III-lysyllysine conjugate decompacts preimplantation mouse embryos, while the free oligosaccharide is ineffective, *J Exp Med* **160**, 1591–6 (1984).

12 Eggens I, Fenderson B, Toyokuni T, Dean B, Stroud M, Hakomori S, Specific Interaction between Le^x and Le^x determinants. A possible basis for cell recognition in preimplantation embryos and in embryonal carcinoma cells, *J Biol Chem* **264**, 9476–84 (1989).

13 Iozzo RV, Matrix proteoglycans: From molecular design to cellular function, *Annu Rev Biochem* **67**, 609–52 (1998).

14 Truant S, Bruyneel E, Gouyer V, De Wever O, Pruvot FR, Mareel M, Huet G, Requirement of both mucins and proteoglycans in cell-cell dissociation and invasiveness of colon carcinoma HT-29 cells, *Int J Cancer* **104**, 683–94 (2003).

15 Humphreys T, Chemical dissolution and *in vitro* reconstruction of sponge cell adhesions. Isolation and functional demonstration of the components involved, *Dev Biol* **8**, 27–47 (1963).

16 Wilson HV, On some phenomena of coalescence and regeneration in sponges, *J Exp Zool* **5**, 245–58 (1907).

17 Crossin KL, Cell adhesion molecules activate signaling networks that influence proliferation, gene expression, and differentiation, *Ann NY Acad Sci* **961**, 159–60 (2002).

18 Cavallaro U, Christofori G, Cell adhesion and signalling by cadherins and Ig-CAMs in cancer, *Nat Rev Cancer* **4**, 118–32 (2004).

19 Férnandez-Busquets X, Burger MM, Circular proteoglycans from sponges: First members of the spongican family, *Cell Mol Life Sci* **60**, 88–112 (2003).

20 Henkart P, Humphreys S, Humphreys T, Characterization of sponge aggregation factor. A unique proteoglycan complex, *Biochemistry* **12**, 3045–50 (1973).

21 Müller WE, Beyer R, Pondeljak V, Müller I, Zahn RK, Species-specific aggregation factor in sponges. XIII. Entire and core structure of the large circular proteid particle from *Geodia cydonium*, *Tissue Cell* **10**, 191–9 (1978).

22 Jarchow J, Fritz J, Anselmetti D, Calabro A, Hascall VC, Gerosa D, Burger MM, Fernandez-Busquets X, Supramolecular structure of a new family of circular proteoglycans mediating cell adhesion in sponges, *J Struct Biol* **132**, 95–105 (2000).

23 Misevic GN, Burger MM, The species-specific cell-binding site of the aggregation factor from the sponge *Microciona prolifera* is a highly repetitive novel glycan containing glucuronic acid, fucose and mannose, *J Biol Chem* **265**, 20577–84 (1990).

24 Misevic GN, Burger MM, Carbohydrate-carbohydrate interactions of a novel acidic glycan can mediate sponge cell adhesion, *J Biol Chem* **268**, 4922–9 (1993).

25 Turner SR, Burger MM, Involvement of carbohydrate group in the active site for surface guided reassociation of animal cells, *Nature* **244**, 509–10 (1973).

26 Jumblatt JE, Schlup V, Burger MM, Cell-cell recognition: Specific binding of Microciona sponge aggregation factor to homotypic cells and the role of calcium ions, *Biochem* **19**, 1038–42 (1980).

27 Spillmann D, Thomas-Oates JE, van Kuik JA, Vliegenthart JF, Misevic G, Burger MM, Finne J, Characterization of a novel sulfated carbohydrate unit implicated in the carbohydrate-carbohydrate-mediated cell aggregation of the marine sponge *Microciona prolifera*, *J Biol Chem* **270**, 5089–97 (1995).

28 Spillmann D, Hard K, Thomas-Oates J, Vliegenthart JF, Misevic G, Burger MM, Finne J, Characterization of a novel pyruvylated carbohydrate unit implicated in the cell aggregation of the marine sponge *Microciona prolifera*, *J Biol Chem* **268**, 13378–87 (1993).

29 Haseley SR, Vermeer HJ, Kamerling JP, Vliegenthart JFG, Carbohydrate self-recognition mediates marine sponge cellular adhesion, *PNAS* **98**, 9419–24 (2001).

30 Beeley JG, Structural analysis. In *Glycoprotein and Proteoglycan Techniques* (Elsevier Science Publishers, Amsterdam, 1989), pp. 153–296.

31 Chon JWM, Mulvaney P, Sader JE, Experimental validation of theoretical models for the frequency response of atomic force microscope cantilever beams immersed in fluids, *J Appl Phys* **87**, 3978–88 (2000).

32 Müller DJ, Baumeister W, Engel A, Controlled unzipping of a bacterial surface layer with atomic force microscopy, *Proc Natl Acad Sci* USA **96**, 13170–4 (1999).

33 Dammer U, Popescu O, Wagner P, Anselmetti D, Guntherodt HJ, Misevic GN, Binding strength between cell adhesion proteoglycans measured by Atomic Force Microscopy, *Science* **267**, 1173–5 (1995).

34 Hinterdorfer P, Baumgartner W, Gruber HJ, Schilcher K, Schindler H, Detection and localization of individual antibody-antigen recognition events by atomic force microscopy, *Proc Natl Acad Sci USA* **93**, 3477–81 (1996).

35 Saleh OA, Sohn LL, Direct detection of antibody-antigen binding using an on-chip artificial pore, *Proc Natl Acad Sci USA* **100**, 820–4 (2003).

36 Tromas C, Rojo J, de la Fuente JM, Barrientos AG, Garcia R, Penades S, Adhesion forces between $Lewis^x$ determinant antigens as measured by atomic force microscopy, *Angew Chem Int Ed* **40**, 3052–5 (2001).

37 Misevic GN, Finne J, Burger M, Involvement of carbohydrates as multiple low affinity interaction sites in the self-association of the aggregation factor from the marine sponge Microciona prolifera, *J Biol Chem* **262**, 5870–7 (1987).

38 Spillmann D, Carbohydrates in cellular recognition: From leucine-zipper to sugar-zipper?, *Glycoconj J* **11**, 169–71 (1994).

39 Guerardel Y, Czeszak X, Sumanovski L, Karamanos Y, Popescu O, Strecker G, Misevic GN, Molecular fingerprinting of carbohydrate structures phenotypes of three porifera proteoglycan-like glyconectins, *J Biol Chem* **279**, 15591–603 (2004).

40 Perez S, Mouhous-Riou N, Nifant'ev NE, Tsvetkov YE, Bachet B, Imberty A, Crystal and molecular structure of a histo-blood group antigen involved in cell adhesion: The Lewis x trisaccharide, *Glycobiology* **6**, 537–42 (1996).

41 Cao Z, Zhao Z, Mohan R, Alroy J, Stanley P, Panjwani N, Role of the Lewis^x glycan determinant in corneal epithelial cell adhesion and differentiation, *J Biol Chem* **276**, 21714–23 (2001).

42 de La Fuente JM, Barrientos AG, Rojas TC, Rojo J, Canada J, Fernandez A, Penades S, Gold glyconanoparticles as water-soluble polyvalent models to study carbohydrate interactions, *Angew Chem Int Ed Engl* **40**, 2257–61 (2001).

43 Spillmann D, Burger MM, Carbohydrate/carbohydrate interactions. In *Oligosaccharides in Chemistry and Biology*, *A Comprehensive Handbook* (Wiley-VCH Verlag GmbH, Weinheim, 2000), pp. 1061–91.